J. Membrane Biol. 105, 221–231 (1988)

The Journal of
Membrane Biology

Ca^{2+}-Activated K^+ Currents in *Necturus* Choroid Plexus

Donald D.F. Loo, Peter D. Brown*, and Ernest M. Wright
Department of Physiology, UCLA School of Medicine, Los Angeles, CA 90024-1751

Summary. The tight-seal whole-cell recording method has been used to study *Necturus* choroid plexus epithelium. A cell potential of -59 ± 2 mV and a whole cell resistance of 56 ± 6 MΩ were measured using this technique. Application of depolarizing step potentials activated voltage-dependent outward currents that developed with time. For example, when the cell was bathed in 110 mM NaCl Ringer solution and the interior of the cell contained a solution of 110 mM KCl and 5 nM Ca^{2+}, stepping the membrane potential from a holding value of -50 to -10 mV evoked outward currents which, after a delay of greater than 50 msec, increased to a steady state in 500 msec. The voltage dependence of the delayed currents suggests that they may be currents through Ca^{2+}-activated K^+ channels. Based on the voltage dependence of the activation of Ca^{2+}-activated K^+ channels, we have devised a general method to isolate the delayed currents. The delayed currents were highly selective for K^+ as their reversal potential at different K^+ concentration gradients followed the Nernst potential for K^+. These currents were reduced by the addition of TEA^+ to the bath solution and were eliminated when Cs^+ or Na^+ replaced intracellular K^+. Increasing the membrane potential to more positive values decreased both the delay and the half-times ($t_{1/2}$) to the steady value. Increasing the pipette Ca^{2+} also decreased the delay and decreased $t_{1/2}$. For instance, when pipette Ca^{2+} was increased from 5 to 500 nM, the delay and $t_{1/2}$ decreased from values greater than 50 and 150 msec to values less than 10 and 50 msec. We conclude that the delayed currents are K^+ currents through Ca^{2+}-activated K^+ channels.

At the resting membrane potential of -60 mV, Ca^{2+}-activated K^+ channels contribute between 13 to 25% of the total conductance of the cell. The contribution of these channels to cell conductance nearly doubles with membrane depolarization of 20–30 mV. Such depolarizations have been observed when cerebrospinal fluid (CSF) secretion is stimulated by cAMP and with intracellular Ca^{2+}. Thus the Ca^{2+}-activated K^+ channels may play a specific role in maintaining intracellular K^+ concentrations during CSF secretion.

Key Words choroid plexus · calcium-activated potassium currents · cerebrospinal fluid secretion · calcium · delayed currents · patch clamp

Introduction

It is well established that cerebrospinal fluid (CSF) potassium (K^+) concentrations are carefully maintained and protected against any changes in plasma K^+ concentration (Pappenheimer, 1967; Bradbury & Kleeman, 1967; Cohen, Gerschenfeld & Kuffler, 1968). The ventricular or apical membrane of choroid plexus epithelium is highly permeable to K^+ (Zeuthen & Wright, 1981). This appears to be important to CSF secretion, acting as a leak pathway for K^+ pumped into the cell by the Na^+/K^+ pump, which is also located in the apical membrane. The control of this permeability would therefore be important to the maintenance of intracellular K^+ concentrations as well as being instrumental in the regulation of transepithelial K^+ fluxes.

In the previous study (Brown et al., 1988) Ca^{2+}-activated K^+ channels with a high conductance (150 pS) were identified in the apical membrane of *Necturus* choroid plexus epithelium. The open probability of the channels was increased by intracellular Ca^{2+}, pH and by depolarizing membrane potentials. They were highly selective for K^+ over Na^+ and Cs^+, and were blocked by both Ba^{2+} and TEA^+ (tetraethylammonium).

Ca^{2+}-activated K^+ channels have been commonly found in the membrane of epithelial cells containing Na^+ pumps (Petersen & Maruyama, 1984; Sepulveda & Mason, 1985; Petersen, 1986). It has been suggested that they act as a leak pathway for the Na^+ pump and contribute a large proportion of K^+ conductance to this membrane.

In this study, the tight-seal whole-cell recording patch-clamp method has been used to study the Ca^{2+}-activated K^+ currents present in epithelial cells from *Necturus* choroid plexus. With depolarizing voltage steps currents through Ca^{2+}-activated K^+ channels activate after a delay. Based on the activation of the Ca^{2+}-activated K^+ channels with membrane depolarization, a general method is de-

* *Present address:* Department of Physiological Sciences, University of Manchester, Manchester M13 9PT, United Kingdom.

scribed to isolate these currents and determine their contribution to whole-cell conductance. A preliminary account of some of this work has appeared (Brown, Loo & Wright, 1987).

Methods

The choroid plexus from the third ventricle of *Necturus maculosa* was isolated and pinned to the bottom of a transparent chamber as previously described (Brown et al., 1988). All the data presented in the present study was performed on intact epithelial tissue except for the experiments to measure membrane capacitance and resting whole-cell resistance. There, isolated cells with actively beating cilia were patched. The cells were isolated from the epithelium by incubating the intact tissue for 60 min under gentle agitation in a solution containing (mM): 25 sodium citrate, 30 NaCl, 10 $NaHCO_3$, 1 dithiothreitol, 0.5 β-OH-butyrate and 10 HEPES (titrated with NaOH to pH 7.3). Bovine serum albumen was also added to the incubating medium at a concentration of 2 mg/ml.

The tissue was normally bathed in a NaCl Ringer solution containing (mM): Na^+, 110; K^+, 2; Ca^{2+}, 1; Mg^{2+}, 1; Cl, 118 buffered with 10 mM HEPES/NaOH at pH 7.3. Where stated, 9 mM NaCl was replaced by an extra 9 mM KCl, resulting in a total K^+ of 11 mM, to study the selectivity of the whole-cell currents.

Patch-clamp electrodes with tip resistances of 2–10 MΩ were pulled from VWR Blue Tip hematocrit capillary and Corning 7052 glass and coated with Sylgard. The electrodes were filled with a pipette solution containing (mM): K^+, 110; Na^+, 1; Mg^{2+}, 1; and Cl^-, 113. In certain experiments, all pipette KCl were replaced by CsCl or NaCl. All pipette solutions were buffered with HEPES at pH 7.3, which is close to the intracellular pH of 7.24 of *Necturus* choroid plexus (Zeuthen, 1987). Three Ca^{2+} activities, 5, 100, and 500 nM were used for pipette solutions. The solutions were prepared using Ca^{2+}-EGTA buffers as described in Brown et al. (1988): 1 mM $CaCl_2$ and 10 mM EGTA were added to obtain 5 nM Ca^{2+}; 6.01 mM $CaCl_2$ and 10 mM EGTA to obtain 100 nM Ca^{2+}; and 1.16 mM $CaCl_2$ and 1.34 mM EGTA to obtain 500 nM Ca^{2+}.

Data Analysis

Whole-cell currents were measured using a patch-clamp amplifier as previously described (Brown et al., 1988). Data were acquired and analyzed using an IBM personal computer interfaced to the Tecmar Labmaster data acquisition system. The computer program, "Pclamp" (Axon Instruments, Burlingame, CA), was used to issue the command signals to the patch-clamp amplifier and to control the data acquisition and for data analysis.

Whole-cell recordings were made by first obtaining a GΩ seal. For cells in the intact tissue, the seal was made on the apical membrane. In the cell-attached configuration, the pipette and the patch-membrane capacitances were compensated for using the capacity compensation of the patch-clamp amplifier. The patch was held at a pipette potential (V_p) of −50 mV (close to the cell potential) as suction was applied to the pipette to rupture the patch membrane. Initiation of the whole-cell recording configuration was marked by a large change in membrane capacitance. Most of the experiments took advantage of the equilibration of the intracellular contents with the pipette solution. This provided well-defined intracellular conditions for each experiment. In addition, initial values of cell resistance and membrane potential corresponding to the resting values were also measured during the first few seconds of the whole-cell recording. Cells were then allowed to equilibrate with the pipette solution before new steady-state parameters were measured.

Whole-cell current-voltage (I–V) relationships were obtained using the Fetchex program (Axon Instruments). This applied a series of step potentials from a defined holding potential (V_h). The potential steps lasted either 50, 450, or 500 msec. Each voltage step was followed by two sec at the holding potential (V_h). The recorded currents were analyzed using the program Clampan (Axon Instruments), and whole-cell I–V relationships were determined. The resistances measured were obtained as the reciprocal of the slope conductance.

To determine the membrane capacitance, only those cells where the pipette and patch capacitances had been compensated for in the cell-attached configuration were used. In the whole-cell recording mode, small (in general, 1–5 mV) positive or negative voltage steps (V_m) were applied from the holding potential of 0 mV for 30 msec. The cell capacitance (C_m) was estimated from the integral of the current transients according to the formula (Adrian, & Almers, 1974)

$$C_m = [I(t_{ss}) - I_{ss} \cdot t_{ss}]/V_m.$$

$I(t_{ss})$ is the integral of the current from the onset of the voltage pulse ($t = 0$) to a time ($t = t_{ss}$, typically 10 msec) where the steady value I_{ss} was reached.

Statistical values are expressed as mean ± SEM.

Results

Cell Potential, Conductance, and Capacitance

Values for the resting-cell potential and whole-cell resistance were obtained before the cell equilibrated with the pipette solution (less than 30 msec after the whole-cell recordings were established). The whole-cell resistance, obtained as the reciprocal of the slope conductance at the reversal potential, was 56 ± 6 MΩ (n = 13). This value is somewhat higher than the input resistance measured by conventional microelectrodes in *Necturus* choroid plexus (22 MΩ, Y. Saito, *unpublished data*) and in bullfrog choroid plexus (33 MΩ, Saito & Wright, 1984). The resting potential was found to be −59 ± 2 mV (n = 13). This is somewhat lower than the apical membrane potential of −87 mV obtained by Zeuthen et al. (1987) using microelectrodes for cells in the fourth ventricle of *Necturus* choroid plexus.

Values for membrane capacitance can be used to indicate the membrane surface area. In seven experiments, the value for capacitance obtained was 20 ± 6 pF (n = 7). Using the standard equivalence of 1 μF to 1 cm^2, the membrane capacitance corresponds to spherical cells with mean diameters of 23 ± 4 μm (n = 7). This is in agreement with the

diameters of the cells (~20 μm) as viewed under the light microscope.

In experiments on cells isolated from the same tissue, the capacitance was 16 ± 4 pF (n = 12), and the resting resistance was 83 ± 13 MΩ (n = 9). There was no significant difference ($P > 0.6$ by unpaired t test) in the capacitance, and the resistances were similar to the values obtained in the intact preparation. Thus we conclude that currents measured in the intact tissue are from single cells. This result is in agreement with Saito and Wright (1983) who found very little cell-to-cell coupling in the cells in the fourth ventricle of the bullfrog choroid plexus.

Equilibration of Pipette and Intracellular Contents

In the following, all the data presented will be from studies on cells in the intact tissue where GΩ seals were made on the apical surface. In this cell-attached configuration, the patch was then held at a pipette potential of −50 mV as suction was applied to rupture the patch membrane. Once the membrane ruptured, the pipette solution quickly equilibrated with the intracellular contents, indicated by a change in the holding current until establishment of steady state. The process of equilibration was approximately fitted with a single exponential. The mean time constant from seven experiments where the pipette contained 110 mM KCl and 5 nM Ca^{2+} was 0.97 ± 0.07 min^{-1}. The time constants were similar when the pipette was filled with 110 mM KCl (100 nM Ca^{2+}) or 110 mM CsCl (100 nM Ca^{2+}), 1.17 ± 0.21 min^{-1} (n = 4) and 0.69 ± 0.18 min^{-1} (n = 3). In practice between 5–8 min are needed before steady-state conditions are approached.

The process of equilibration was accompanied by changes in the cell conductance. The final steady-state values depended on the pipette Ca^{2+} concentration. When the pipette Ca^{2+} was buffered at 100 nM and 5 nM, the resistance increased above the 56 ± 5 MΩ measured initially before equilibration to 77 ± 15 MΩ (n = 5) and 110 ± 31 MΩ (n = 3). The increases in resistance at the membrane potential of −60 mV in pairwise comparisons were 35 ± 13% (n = 5) and 108 ± 21% (n = 3); whereas, with the pipette solution buffered at 500 nM Ca^{2+}, the resistance decreased to 35 ± 4 MΩ (n = 4), and the decrease in individual cell resistance (at V_m = −60 mV) was 73 ± 4% (n = 4). The steady-state values for whole-cell resistance measured with 5, 100, and 500 nM Ca^{2+} in the pipette solution are shown in Table 1*A*. Comparison of these values suggests that the intracellular Ca^{2+} under resting conditions lies between 100 and 500 nM. Furthermore, if the steady-state conductance at 5 nM is assumed to be the Ca^{2+}-independent conductance of the cell, then the difference between this value and that measured initially before equilibration indicates that intracellular Ca^{2+} can control as much as 50% of the total resting conductance of the cell. This estimate is an upper limit as it assumes that no intracellular regulatory factors other than Ca^{2+} are lost during dialysis of the cell interior.

Table 1. Steady-state whole-cell resistance (R)

A) Ca^{2+} sensitivity

Pipette Ca^{2+} (nM)	R (−60 mV) (10^6 Ω)	Change (%)	n
5	110 ± 31	108 ± 21	3
100	77 ± 15	35 ± 13	5
500	35 ± 4	−73 ± 4	4

B) Cation selectivity

Pipette cation (110 mM)	R (10^6 Ω) −60 mV	−10 mV	n
K^+	77 ± 15	68 ± 11	5
Cs^+	86 ± 10	118 ± 25	3
Na^+	86 ± 5	111 ± 16	3

Results were obtained once the exchange between intracellular contents reached a steady state. They were determined at V_m = −60 mV in *A* and at −60 and −10 mV in *B* and are expressed as mean ±SEM. The percentage change in cell resistance at V_m = −60 mV from the initial value determined before initiation of equilibration to the values obtained after steady-state conditions was established. The values shown are from paired experiments. The minus (−) sign represents a decrease in cell resistance. The pipette solution in *A* contained 110 mM K^+ while the Ca^{2+} was varied. In *B*, the pipette solution contained 100 nM Ca^{2+} and the cation was varied.

Whole-Cell I–V Relationships: General Characteristics

Whole-cell I–V relationships were studied after steady-state conditions had been established (~8 min). From an initial holding potential (V_h) the membrane potential was stepped to a number of new potentials (depolarizing and hyperpolarizing) for periods of up to 500 msec. Typical current traces recorded for such an experiment with V_h = −50 mV and with the pipette solution contained 110 mM KCl and 5 nM Ca^{2+} are shown in Fig. 1*A*.

In response to hyperpolarizing voltage steps, there was a rapid transient, with a time constant of approximately 4 msec, to the steady state. These consisted of capacitative and background currents.

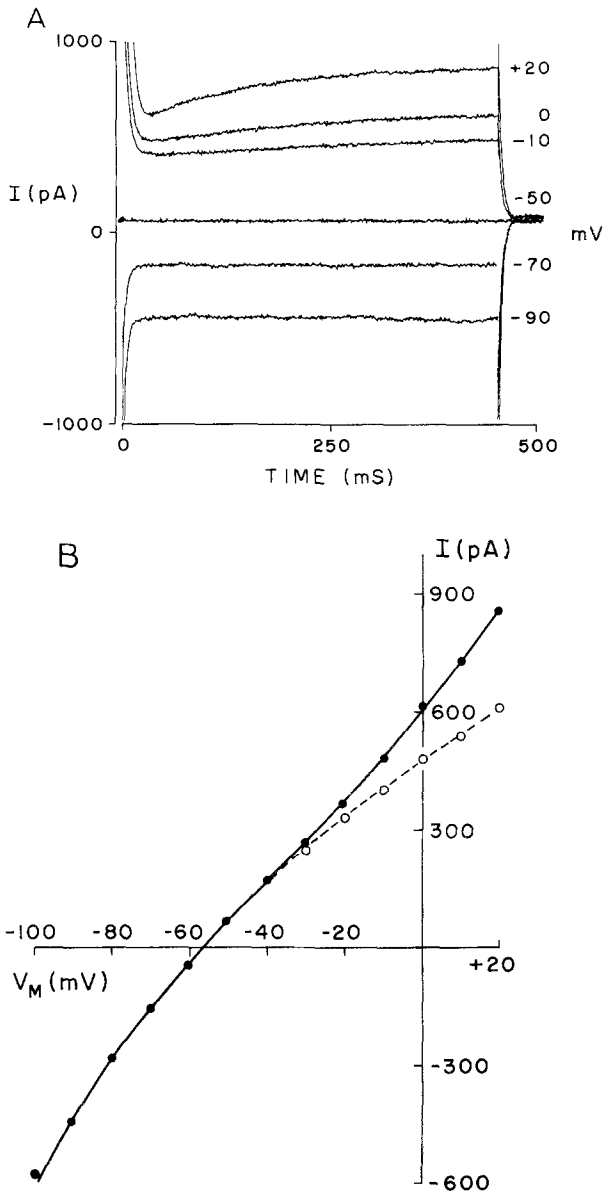

Fig. 1. (*A*) Whole-cell current records for choroid plexus epithelial cells. The cell was held at $V_h = -50$ mV, and step potentials (hyperpolarizing and depolarizing) were applied for 450 msec. The numbers to the right of each trace indicate the potential step applied. (*B*) Whole-cell *I–V* relationships. Steady-state (●) and "instantaneous" (○) currents measured at 450 and 25 msec are plotted. The lines joining the points were fitted by eye. Pipette solution was 110 mM KCl (5 nM Ca^{2+}), and the bath contained NaCl Ringer

When the voltage steps were positive, there was a similar rapid transient to the steady state. However, as the size of the depolarizing voltage steps was made larger, after the decrease of the initial transients to steady state (in 25 msec), there was a subsequent rise to a new steady state after 400 msec (Fig. 1*A*). The size of these delayed currents increased with increasing depolarizations. They were completely absent at membrane potentials more negative than −40 mV. The *I–V* relationships for the current traces measured before (25 msec) and after the development of the rising currents (450 msec) are plotted in Fig. 1*B*. For the experiment of Fig. 1, where the pipette Ca^{2+} was 5 nM, the rising currents made up 10% of the total steady-state currents at $V_m = -10$ mV (Fig. 1*B*). It is these rising currents that are the subject of the remainder of this paper.

Isolation and Identification of the Delayed Currents

The activation of the delayed rising currents with depolarizing membrane potentials suggests that they may be currents through Ca^{2+}-activated K^+ channels, the latter also activated by depolarizing potentials (Brown et al., 1988). Based on the voltage dependence of the activation of Ca^{2+}-activated K^+ channels, we have devised a method to isolate the current through these channels. We first hold the membrane at a large negative potential where the channels are closed. Under this condition the "instantaneous" *I–V* relationships, that is, the currents measured 25 msec from the onset of the voltage step and prior to the opening of the K^+ channels, are the background currents. The holding potential is then changed to a value where the Ca^{2+}-activated K^+ channels are open. Here the "instantaneous" *I–V* relationships consist of background currents and currents going through Ca^{2+}-activated K^+ channels. Hence, pointwise subtraction of the two *I–V* relationships would yield the K^+ currents. An example of such an experiment is shown in Fig. 2. The pipette contained 110 mM K^+ and 5 nM Ca^{2+}; the bath solution was 110 mM NaCl Ringer with 11 mM KCl. The holding potential where the Ca^{2+}-activated K^+ channels were expected to be closed was −50 mV, and the potential at which the channels were expected to be open was chosen to be −10 mV. The currents corresponding to stepping the potentials in a depolarizing or hyperpolarizing direction from the two holding potentials, −10 mV (Fig. 2*B*) and −50 mV (Fig. 2*A* and *C*), are shown in the left panels. The step potentials, indicated by the numbers to the right of each current trace, were applied for 45 msec. These experiments were performed in sequence (*A–C*) within a 9-min period. Each trace shows the decay of the initial transient current to the steady state. The *I–V* relationships measured at 45 msec after the onset of the voltage pulse are indicated in the right panels (Fig. 2).

At $V_h = -50$ mV (Fig. 2*A* and *C*), the *I–V*

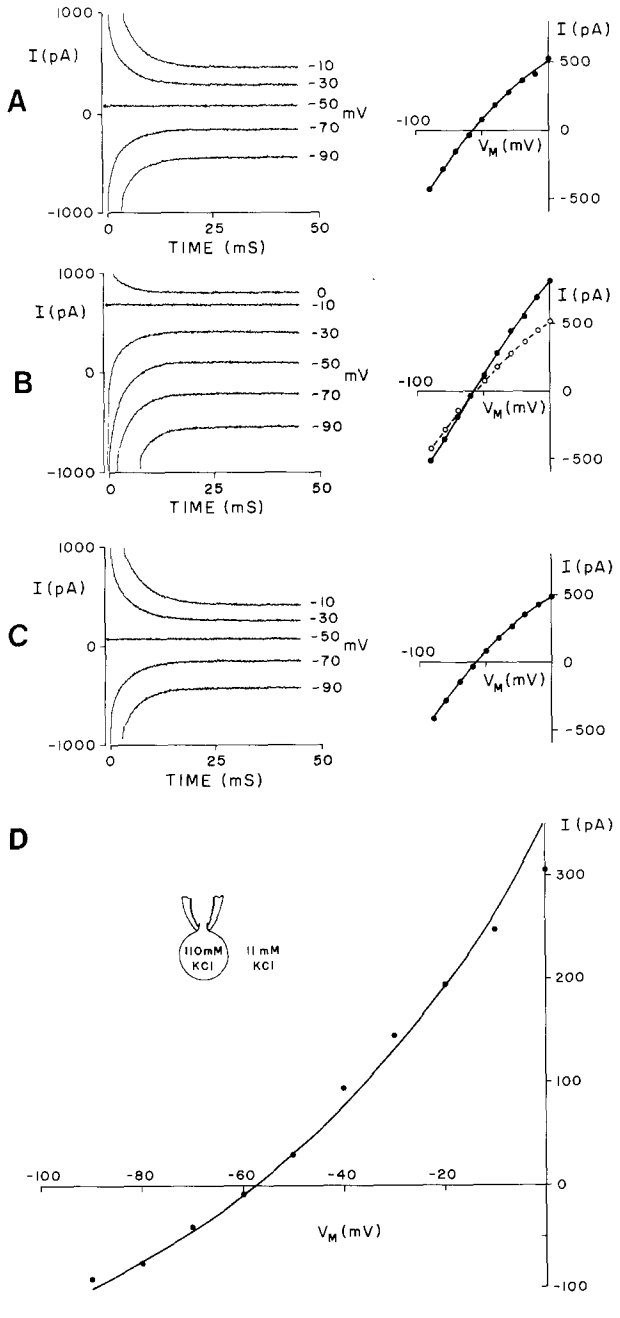

Fig. 2. "Instantaneous" whole-cell current traces and *I–V* relationships. The cell was held at (*A*) −50 mV, (*B*) −10 mV, and (*C*) −50 mV over the course of the experiment. Voltage steps were applied for 45 msec from each holding potential. Current traces are shown in the left-hand panel, and the "instantaneous" *I–V* relationships (currents, ●, measured at 25 msec) are plotted to the right. The lines joining the currents are fitted by eye. The second dashed line in *B* joins the mean current (○) from *A* and *C*. (*D*) shows the instantaneous *I–V* relationships for the delayed current. The currents (●) were the differences between the "instantaneous" *I–V* relationships measured with reference to V_h = −50 (●, Fig. 2*B*) and −10 mV (○, Fig. 2*B*). The curve was drawn according to Eq. (1) with K_o = 11 mM, K_i = 110 mM, and P_K = 36 × 10^{-12} $cm^3 \cdot sec^{-1}$ per cell. In this experiment, the pipette solution was 110 mM KCl (5 nM Ca^{2+}), and the bath contained NaCl Ringer solution with 11 mM KCl

curves showed an inward rectification (greater inward than outward current). In order to minimize any drifts that might occur within the course (9 min) of the experiment, the currents measured at each potential from Fig. 2*A* and *C* were averaged. In this particular experiment, there was very little difference between the two *I–V* relationships measured at the beginning (*A*) and the end (*C*) of the experiment. These mean currents measured from V_h = −50 mV are shown (○) in Fig. 2*B*. This curve serves to emphasize the differences between the *I* − *V* measured at the two holding potentials, V_h = −10 mV (Fig. 2*B*, ●) and V_h = −50 mV (Fig. 2*B*, ○).

The differences between the currents measured at the two holding potentials (Fig. 2*B*) are plotted in Fig. 2*D*, which is the "instantaneous" *I–V* relationship for the delayed activating current at V_h = −10 mV. Hence we have described a method for the isolation of the delayed currents based on the voltage dependence of the Ca^{2+}-activated K^+ channels. Using this method we have characterized these currents with respect to their selectivity, dependence on intracellular Ca^{2+}, and blockage by TEA^+.

Selectivity for K^+ Cs^+ and Na^+

Selectivity of the delayed currents for K^+ was studied by determining the reversal potentials at different K^+ concentration gradients across the cell. In our experiments the pipette KCl concentration was kept constant at 110 mM while bath K^+ concentrations were varied. The results from such an experiment are shown in Fig. 3, where the bath solution contained 2 mM KCl. The currents were the difference between the "instantaneous" *I–V* relationships measured at the two holding potentials −70 and −30 mV. In Fig. 3, the reversal potential was close to the calculated Nernst potential of −102 mV for K^+. Similar observations were obtained in eight other experiments.

Changing the bath K^+ concentration shifted the reversal potential in the direction expected for a current that is highly selective for K^+. For instance, when bath K^+ was increased from 2 to 11 mM, the reversal potential was close to the Nernst potential of −58 mV for K^+ (Fig. 2*D*).

The line in Fig. 3 shows the fit of the data to Eq. (1) (Hodgkin & Katz, 1949)

$$I_K = [P_K \cdot F^2V/RT][K_o - K_i \exp(VF/RT)]/[1 - \exp(VF/RT)]. \quad (1)$$

Where K_o and K_i are the bath and pipette K^+ concentrations and P_K is the K^+ permeability coefficient. This equation has previously been found to fit

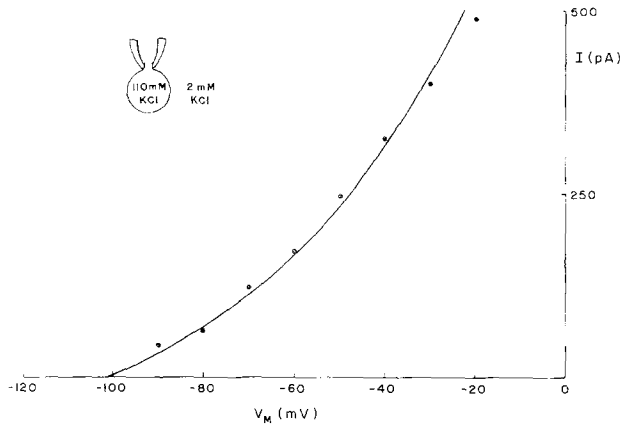

Fig. 3. *I–V* relationships for the delayed component of the whole-cell conductance. The currents shown are the differences between the "instantaneous" *I–V* relationships measured with reference to the holding potentials of $V_h = -70$ and -30 mV. The curve was drawn through the data using the equation

$$I_K = [P_K \cdot F^2 V_m / RT][K_o - K_i \exp(V_m F/RT)]/[1 - \exp(V_m F/RT)].$$

Where F, R and T have their usual meanings. V_m is the membrane potential. K_o = 2 mM and K_i = 110 mM are the bath and pipette K^+ concentrations and $P_K = 80 \times 10^{-12}$ cm^3 · sec^{-1} per cell. The pipette solution was 110 mM KCl (5 nM Ca^{2+}), and the bath was NaCl Ringer solution with 2 mM K^+. The calculated K^+ reversal potential was -102 mV

the single-channel *I–V* relationships for Ca^{2+}-activated K^+ channels in *Necturus* choroid plexus (Brown et al., 1988), and it can be seen that the delayed currents are also well described by this equation in the range of potentials (-110 to 20 mV) studied. The permeability coefficient P_K for the line was 80×10^{-12} cm^3 · sec^{-1} per cell.

P_K, the K^+ permeability coefficient was dependent on the membrane potential V_m. In five experiments where the pipette Ca^{2+} was 100 nM with 110 mM KCl and the bath solution was 110 mM NaCl and 2 mM KCl, values for P_K (obtained with reference to $V_h = -70$ mV) were 21 ± 9 ($n = 2$) and $43 \pm 4 \times 10^{-12}$ cm^3 · sec^{-1} per cell ($n = 3$) at $V_m = -50$ and -30 mV. This dependence on voltage was consistent with the dependence of open probability of Ca^{2+}-activated K^+ channels on membrane potential (Brown et al., 1988).

In single-channel experiments, Na^+ and Cs^+ were found to be impermeant to the Ca^{2+}-activated K^+ channels (Brown et al., 1988). Thus, the selectivity of the delayed currents for Cs^+ and Na^+ were examined by the replacement of the pipette KCl by either CsCl or NaCl. Figure 4 shows the currents and *I–V* relationship for an experiment in which the pipette solution contained 110 mM CsCl and the bath contained 110 mM NaCl. The current traces

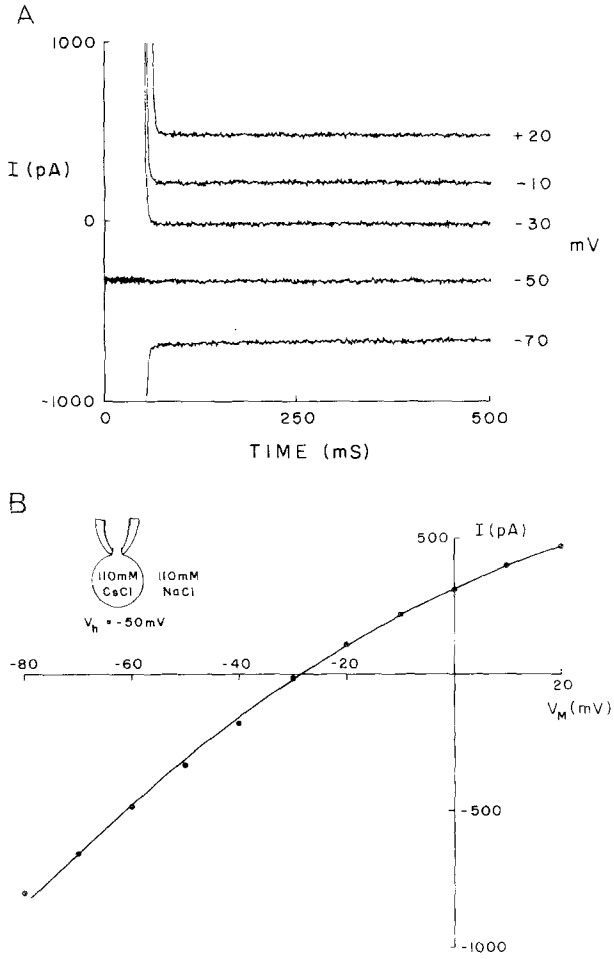

Fig. 4. (*A*) Whole-cell current traces and (*B*) *I–V* relationships with intracellular Cs^+. The cell was allowed to equilibrate with a pipette solution in which K^+ had been replaced by 110 mM Cs^+ (5 nM Ca^{2+}). The cell was held at $V_h = -50$ mV, and step potentials (indicated to the right) were applied for 450 msec. The currents measured after 450 msec (●) are plotted against V_m in 4*B*. Bath solution was 110 mM NaCl Ringer solution

(Fig. 4*A*) at both hyperpolarizing and depolarizing potentials show the initial transients as when the pipette solution contained KCl; however, the delayed rising currents have been completely abolished. The currents quickly reached a plateau in 20 msec at which they are stable for the remainder of the voltage pulse. These results were observed in all six experiments studied with the pipette filled with CsCl, and similar results were observed in four experiments when Na^+ replaced pipette K^+. These results indicate that the channels responsible for the delayed currents are highly selective for K^+ over Na^+ and Cs^+.

Fig. 4*B* is an *I–V* plot of the currents measured after 500 msec for each step potential. The shape of the curve showing inward rectification for the volt-

Table 2. Total and delayed currents measured at a depolarizing potential (−10 mV)[a]

Ca^{2+} (nM)	Total current (pA)	Delayed current (pA)	% Delayed current	n
5	407 ± 21	37 ± 8	9.1 ± 2.4	3
100	550 ± 167	80 ± 40	11.9 ± 3.9	5
500	832 ± 103	145 ± 35	17.2 ± 4.2	4
Resting	620 ± 83	97 ± 42	14.4 ± 4.7	4

[a] Experiments were performed at three Ca^{2+} (5, 100, and 500 nM) concentrations and before the equilibration with the pipette solution (resting). The cell was held at −50 mV, and a depolarizing step to −10 mV was then applied for 450 msec. The total current was measured after a new steady-state current was established (450 msec). The delayed current was calculated by subtracting the "instantaneous" current measured after ~25 msec from the total current. Values for the change in delayed current were from paired experiments. The pipette solution contained 110 mM K^+, and the bath solution was NaCl Ringer in each case.

age range studied (−100 to +20 mV) is similar to that in Fig. 2*A* and *C*, where the delayed current was inactive. This inward-rectifying *I–V* relationship therefore represents the background or baseline currents. The similarities between the "instantaneous" *I–V* relationships in the presence of K^+ (Fig. 2*A* and *C*) and the *I–V* relationships when K^+ in the pipette is replaced by Cs^+ (Fig. 4*B*) and Na^+ (*data not shown*), suggest that the background conductances are nonspecific to K^+, Cs^+, and Na^+ and are probably Cl^- currents or nonspecific "leak" currents.

Table 1*B* summarizes the steady-state resistance values at V_m = −60 and −10 mV after cells had equilibrated with pipette solutions in which K^+ had been replaced by 110 mM Na^+ or 110 mM Cs^+ (Ca^{2+} = 100 nM). In both cases, at V_m = −60 mV, the replacement of the pipette K^+ caused the whole-cell resistance to increase above that obtained with 110 mM K^+ (77 MΩ), to 86 MΩ with Na^+ and Cs^+. The increases in the individual cell resistance were 51 ± 26% (n = 3) and 55 ± 20% (n = 3) for Na^+ and Cs^+, respectively. Comparison of these values suggests that at V_m = −60 mV (100 nM Ca^{2+}) the K^+ conductance accounts for 10 to 50% of the cell conductance. The contribution of K^+ to cell conductance increased drastically with depolarization of the membrane potential to −10 mV (Table 1*B*).

Calcium-Activation

In the range of Ca^{2+} studied (5–500 nM), intracellular Ca^{2+} affected both the magnitude and the kinetics of the delayed inward currents. The dependence of the magnitude of the delayed inward currents on intracellular Ca^{2+} is shown in Table 2, which summarizes the contribution of this conductance to the whole-cell current at V_h = −10 mV at three Ca^{2+} concentrations, 5, 100, and 500 nM. Both total current and the delayed current increased from 407 to 832 pA and from 37 to 145 pA, respectively, with the same increase in Ca^{2+}. Increasing the intracellular Ca^{2+} increased the percentage of the conductance due to the delayed currents to the total conductance. The fractional contribution of the delayed current to total current nearly doubled from 9.1% of the total current at 5 nM to 17.2% when Ca^{2+} was 500 nM. This increase may be actually larger because at 500 nM Ca^{2+}, the open probability of Ca^{2+}-activated K^+ channels were high (at −50 mV), and the currents through these channels contribute to a significant portion of the "instantaneous" current.

When pipette K^+ was replaced by Cs^+, there was no significant effect of pipette Ca^{2+} upon the whole-cell conductance. In Cs^+ containing pipette solutions, increasing pipette Ca^{2+} from 100 nM to 500 nM decreased whole-cell resistance slightly from 94 ± 18 MΩ (n = 3) to 81 ± 16 MΩ (n = 3). In contrast, in the presence of K^+, the resistance decreased from 77 ± 15 MΩ to 35 ± 4 MΩ as pipette Ca^{2+} increased from 100 nM to 500 nM (*see* Table 1*A*) and provided further evidence that a large proportion of the decrease in whole-cell resistance caused by Ca^{2+} is the result of the activation of the voltage-dependent K^+ current. Thus, it appeared that the background conductance was relatively independent of pipette Ca^{2+}.

The dependence of P_K on intracellular Ca^{2+} was studied in six experiments. P_K at a holding potential of −50 mV, was calculated with a reference potential (V_h) of −70 mV, and was 0, 21 and 38 × 10^{-12} $cm^3 \cdot sec^{-1}$ per cell at 5, 100 and 500 nM Ca^{2+}, respectively. Hence for a cell at a resting potential of −50 mV and assuming intracellular Ca^{2+} between 100 and 500 nM, Ca^{2+}-activated K^+ channels will contribute between 21 × 10^{-12} to 38 × 10^{-12} $cm^3 \cdot sec^{-1}$ per cell of the K^+ permeability.

Ca^{2+} also affected the kinetics of the delayed currents. When pipette Ca^{2+} was 500 nM and step potentials (from a holding potential V_h) were applied for 50 msec, the delayed inward currents were observed after only about 15 msec at the more depolarizing potentials (V_m = −30 to 0 mV). This contrasts with similar experiments, but using 5 nM Ca^{2+} (Fig. 2*A*), where delayed inward currents were rarely observed before 50 msec had elapsed from the application of the step potential. The duration of the delays at various depolarizing potentials from V_h = −50 mV are shown in Fig. 5*A*. Delay was defined as the time interval from the onset of the voltage pulse to the time where the current was

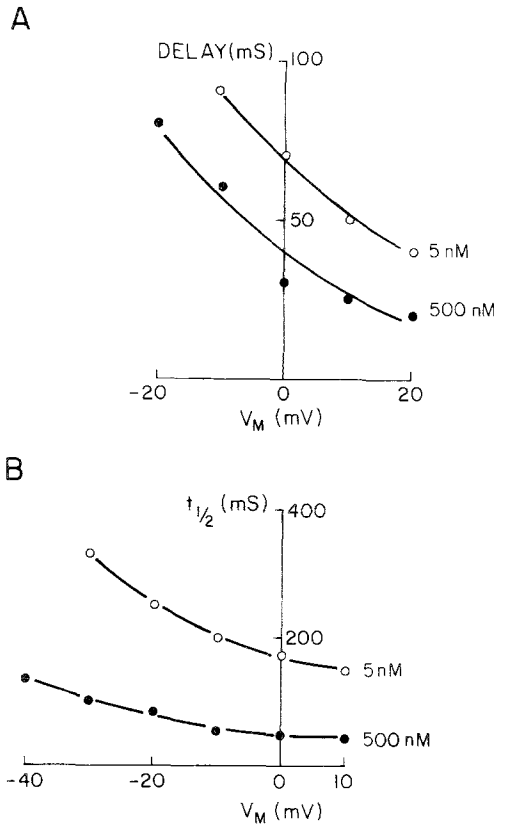

Fig. 5. (*A*) Effects of Ca^{2+} upon the kinetics of delayed inward currents and calcium dependence of delay times. The delays were measured from the onset of voltage pulse at time = 0 until the appearance of the voltage-dependent currents for step potentials from V_h = −50 mV. Values from three experiments in the presence of 500 nM (●) and 5 nM (○) Ca^{2+} are presented. (*B*) Half-times ($t_{1/2}$) for the delayed inward currents. Values were measured from t = 0 to the time ($t_{1/2}$ at which the current was half-maximal, at 500 nM (●) and 5 nM (○) pipette Ca^{2+} in three experiments. Step potentials were applied for 500 msec from V_h = −50 mV. In *A* and *B*, the pipette solution contained 110 mM KCl (with either 5 or 500 nM Ca^{2+}), while the solution was 110 mM NaCl Ringer solution

greater than twice the background peak-to-peak noise in this signal. Values obtained when the pipette Ca^{2+} was 500 (●) and 5 nM (○) are presented. At both concentrations, the length of the delays decreased with the size of the depolarizing steps (e.g., with 500 nM Ca^{2+}, the delays were 80 and 20 msec at depolarizations to V_m = −20 and +20 mV). Increasing pipette Ca^{2+} from 5 nM to 500 nM also caused the length of each delay to decrease. At each of the potentials shown, they were approximately half the length (52 ± 6%, n = 4) of those measured with 5 nM Ca^{2+}.

The reduction in the length of delay observed at 500 nM Ca^{2+} is accompanied by the increased rate at which the voltage-dependent current develops. Figure 5*B* plots the half-times, $t_{1/2}$ (the times from the onset of the voltage pulse to the time where 50% of the steady-state value is reached), with which these currents develop at various depolarizing potentials in the presence of 5 or 500 nM Ca^{2+}. At both Ca^{2+} concentrations, the $t_{1/2}$ decreased with depolarization (e.g., with 5 nM Ca^{2+}, $t_{1/2}$ decreased from 330 msec at V_m = −30 mV to 150 msec at V_m = 10 mV). The Ca^{2+} concentrations also affect $t_{1/2}$ which were reduced by about 70% at each potential when Ca^{2+} increased from 5 to 500 nM.

TEA^+-Sensitivity

TEA^+ blocks Ca^{2+}-activated K^+ channels with a high affinity (K_D (0 mV) = 0.23 mM, Brown et al., 1988) when applied to the outside of the channel. In six experiments in the intact preparation, TEA^+ was added to the bathing solution. The effect of TEA^+ was not immediate as in the case of TEA^+ on Ca^{2+}-activated K^+ channels in isolated membrane patches (Brown et al., 1988) but required long periods to block. The block varied by a 14 to 100% reduction of the delayed outward currents, 7–18 min after application of 1–30 mM TEA^+. TEA^+ had very little effect on the background conductance. At the membrane potential of −90 mV where the delayed currents were negligible, in the course of the experiments above, the background currents were reduced by 8 ± 3% (n = 4).

Discussion

Ca^{2+}-activated K^+ channels have previously been identified in the apical membrane of *Necturus* choroid plexus epithelium (Brown et al., 1988; Christensen & Zeuthen, 1987). These channels are highly selective for K^+ over Na^+ and Cs^+, and are activated by membrane depolarization and intracellular Ca^{2+}. In the present study, the contribution of these channels to the cell conductance is assessed. The opening of the Ca^{2+}-activated K^+ channels was manifested as a delayed increase in outward currents at large depolarizing potentials. The delayed currents are highly specific K^+ over Na^+ or Cs^+ and are reduced by TEA^+. Membrane depolarization and intracellular Ca^{2+} affected the kinetics of current activation in a similar way; they both increased the magnitude and the rate of rise of the currents as well as shortened the delay. Thus, qualitatively at least, the selectivity, voltage dependence and sensitivity to intracellular Ca^{2+} of the delayed outward currents indicate that they are currents through Ca^{2+}-activated K^+ channels.

The sensitivity of the delayed currents for TEA^+ was greatly reduced in the whole-cell experiments as compared to single-channel studies where 2 mM of TEA^+ applied to the outside surface of the patch completely abolished all channel activity (K_D = 0.2 mM, Brown et al., 1988). A similar reduction in the efficiency of TEA^+ for blocking whole-cell currents appeared to be observed by Iwatsuki and Petersen (1985) in pancreatic acinar cells. One explanation for this difference is that the macroscopic currents are through many channels, each of which is rarely open. If TEA^+ blocks only when channels are open, then the affinity of TEA^+ would appear to be reduced. However, we were unable to test this hypothesis because the large currents encountered when channel-open probability was high saturated our patch-clamp amplifier.

Ca^{2+}-activated K^+ currents are distinguished by their delay of activation with membrane depolarization. Several factors could account for the observed delay. One possibility is that the channel must pass through a number of closed configurations before opening. Some of these steps are voltage dependent and involve Ca^{2+} binding. This hypothesis is supported by the kinetic studies of Ca^{2+}-activated K^+ channels from rat muscle (Methfessel & Boheim, 1982; Magleby & Pallota, 1983; Moczydlowski & Latorre, 1983). The observation of the delay being reduced by increasing Ca^{2+} and membrane depolarization is also consistent with this multistate binding hypothesis. However, whether the precise kinetic behavior is identical in whole-cell and single-channel studies remains to be confirmed. Moreover, based on the present experiments, we cannot rule out the possibility that membrane potential may influence intracellular Ca^{2+}. It remains to be studied whether the delay is accountable by the multistate nature of the channel activation or involves changes in the availability of Ca^{2+}.

In the present experiments, 5 to 8 min were required for equilibration between the pipette and cell contents. This rate is comparable to that reported by Maruyama and Petersen (1984) for pancreatic acinar cells; however, it was considerably slower than the value of 15 sec observed by Fenwick, Marty and Neher (1982) for chromaffin cells.

The number of channels per cell (N) can be estimated from knowledge of the permeability coefficients P_K^{chan} for a single Ca^{2+}-activated K^+ channel and the permeability coefficient P_K^{cell} of the Ca^{2+}-activated K^+ currents using the relation $N = P_K^{cell}/P_o P_K^{chan}$ where P_o is the open probability. Since $P_K^{chan} = 4.6 \times 10^{-13}$ cm^3 · sec^{-1} per channel for a 150-pS channel (Brown et al., 1988) and $P_K^{cell} = 10 \times 10^{-13}$ cm^3 · sec^{-1} per cell, for a resting-open probability P_o, of 10^{-4}, this would correspond to 440 channels per cell. The number of channels in the apical membrane can be estimated from the apical membrane area and the density of Ca^{2+}-activated K^+ channels in the apical membrane. In patch-clamp studies on the apical membrane, an average of two channels per patch were observed (Brown et al., 1988), thus the channel density is 0.9 $(\mu m)^2$ of membrane area per channel. In the present study, capacitance measurements indicate that the cells have a surface area of 20×10^{-6} cm^2. If the area occupied by the apical membrane is $\frac{1}{4}$ of this value, then the apical membrane area is 5×10^{-6} cm^2. The number of channels in the apical membrane is 5×10^{-6} cm^2/0.9 $\times$ $(\mu M)^2$ = 560 channels. Thus the two estimates of channel density are similar, suggesting that all of the channels are in the apical membrane. As a comparison, the Ca^{2+}-activated K^+ channels are more dense in choroid plexus than in the pancreatic acinar cell where Maruyama et al. (1983) have estimated a total of 25–60 channels per cell.

The present study indicates that Ca^{2+}-activated K^+ channels contribute between 3.8×10^{-6} and 12.1×10^{-6} cm · sec^{-1} to the K^+ permeability of the apical membrane at $V_m = -50$ mV. At the resting potential and in unstimulated tissue, the contribution of these channels to total conductance is small, ranging from 10 to 25%. We have also found that these are not the only K^+ channels in the apical membrane. In preliminary single-channel studies, we have observed a K^+ channel in up to 20% of the patches, which has an inward-rectifying current-voltage relationship similar to the inward-rectifying I–V relationship of the background conductance. These channels have a maximum conductance of 90 ± 13 pS (n = 7) and are relatively voltage independent with a $P_o = 0.099 \pm 0.027$ (n = 5) at the resting potential (*unpublished data*). These channels may provide for the remaining resting (nonsecreting) basal K^+ conductance of the cell. The relative contribution of these two K^+ channels to resting K^+ conductance remains to be studied. Since the inward-rectifying K^+ channels are voltage independent, a substantially greater contribution can be expected from the Ca^{2+}-activated K^+ channels upon a depolarization to −30 mV where P_K of the Ca^{2+}-activated K^+ currents increased to between 15.1×10^{-6} and 22.5×10^{-6} cm · sec^{-1}. With membrane depolarization, the present findings indicate that the relative contribution of these currents to whole-cell conductance increases significantly, suggesting that they might play a role in physiological conditions where there is a membrane depolarization.

The apical membrane of the choroid plexus accounts for more than 90% of the K^+ conductance of the cell (Zeuthen & Wright, 1981). Since there is

normally a small net transepithelial flux of K^+ from the ventricle to the basolateral side, most of the K^+ pumped into the cell by the Na^+/K^+ pump is reflux back across the apical membrane. Stimulation of the cell by adrenergic agonists, which raise intracellular cyclic-AMP, results in increased CSF secretion (Saito & Wright, 1983). Upon cAMP stimulation, the apical membrane depolarizes, a result of increased Cl^- and HCO_3^- conductances in this membrane (Saito & Wright, 1984). This depolarization activates the Ca^{2+}-activated K^+ currents, which make up a larger share of the conductance of the cell at depolarizing potentials. The significance of the activation of K^+ channels in choroid plexus has not been studied, but it would probably reflect an increase in intracellular K^+, which could be brought about by increased Na^+/K^+ pump activity. The effect of cAMP on a pump rate has not been directly studied, but it is known that the addition of HCO_3^- to the choroid plexus, which increases CSF production on its own, causes pump rate to almost double (Wright, 1977). The Ca^{2+}-activated K^+ channels are tightly regulated by a number of factors. Besides depolarization, intracellular pH and Ca^{2+} may also have a regulating role. Changes in pH may well be important in a tissue where HCO_3^- is of primary importance to the process of secretion. However, their precise contribution remains to be studied; little is known about the cAMP sensitivity of both the Ca^{2+}-activated K^+ and inward-rectifying K^+ channels as well as the changes in intracellular Ca^{2+} and pH upon cAMP stimulation.

Voltage-dependent, depolarization-activated Ca^{2+}-activated K^+ currents have previously been identified in exocrine gland acinar cells (Findlay, 1984; Maruyama & Petersen, 1984; Trautmann & Marty, 1984) and chromaffin cells (Marty & Neher, 1985). Since Ca^{2+}-activated K^+ channels have been identified in almost every cell type studied thus far, the method that we have described may be applicable to other cells.

It is a pleasure to thank Bryndis Birnir and Jeffery Demarest for their critical reading and helpful comments on the manuscript. This work was supported by Grant No. NS09666 from the National Institutes of Health.

References

Adrian, R.H., Almers, W. 1974. Membrane capacity measurements on frog skeletal muscle in media of low ion content. *J. Physiol. (London)* **237:**573–605

Bradbury, M.W.B., Kleeman, C.R. 1967. Stability of the potassium content of cerebrospinal fluid and brain. *Am. J. Physiol.* **213:**519–528

Brown, P.D., Loo, D.D.F., Wright, E.M. 1987. Identification of Ca^{2+} activated K^+ currents in *Necturus* choroid plexus. *J. Physiol. (London)* **390:**70P

Brown, P.D., Loo, D.D.F., Wright, E.M. 1988. Ca^{2+}-activated K^+ channels in the apical membrane of *Necturus* choroid plexus. *J. Membrane. Biol.* **105:**207–219

Christensen, O., Zeuthen, T. 1987. Maxi-K^+ channels in leaky epithelia are regulated by intracellular Ca^{2+}, pH and membrane potential. *Pfluegers Arch.* **408:**249–260

Cohen, M.W., Gerschenfeld, H.M., Kuffler, S.W. 1968. Ionic environment of neurones and glial cells in the brain of an amphibian. *J. Physiol. (London)* **197:**363–380

Fenwick, E.M., Marty, A., Neher, E. 1982. A patch-clamp study of bovine chromaffin cells and of their sensitivity to acetylcholine. *J. Physiol. (London)* **331:**577–597

Findlay, I. 1984. A patch-clamp study of potassium channels and whole-cell currents in acinar cells of the mouse lacrimal gland. *J. Physiol. (London)* **350:**179–195

Hodgkin, A.L., Katz, B. 1949. The effect of sodium ions on the electrical activity of the giant axon of the squid. *J. Physiol. (London)* **108:**37–77

Iwatsuki, N., Petersen, O.H. 1985. Action of tetraethylammonium on calcium-activated potassium channels in pig pancreatic acinar cells studied by patch-clamp single-channel and whole-cell recording. *J. Membrane Biol.* **86:**139–144

Magleby, K.L., Pallota, B.S. 1983. Calcium dependence of open and shut interval distributions from calcium-activated potassium channels in cultured rat muscle. *J. Physiol. (London)* **344:**585–604

Marty, A., Neher, E. 1985. Potassium channels in cultured bovine adrenal chromaffin cells. *J. Physiol. (London)* **367:**117–142

Maruyama, Y., Petersen, O.H. 1984. Control of K^+ conductance by cholecystokinin and Ca^{2+} in single pancreatic acinar cells studied by the patch-clamp technique. *J. Membrane Biol.* **79:**293–300

Maruyama, Y., Petersen, O.H., Flanagan, P., Pearson, G.T. 1983. Quantification of Ca^{2+}-activated K^+ channels under hormonal control in pig pancreas acinar cells. *Nature (London)* **305:**228–232

Methfessel, C., Boheim, G. 1982. The gating of single-calcium-dependent potassium channels is described by an activation/blockade mechanism. *Biophys. Struct. Mech.* **9:**35–60

Moczydlowski, E., Latorre, R. 1983. Gating kinetics of Ca^{2+}-activated K^+ channels from rat muscle incorporated into planar lipid bilayers: Evidence for two voltage-dependent Ca^{2+} binding reactions. *J. Gen. Physiol.* **82:**511–542

Pappenheimer, J.R. 1967. The ionic composition of cerebral extracellular fluid and its relation to control breathing. *Harvey Lect.* **67:**71–94

Petersen, O.H., Maruyama, Y. 1984. Calcium-activated potassium channels and their role in secretion. *Nature (London)* **307:**693–696

Petersen, O.H. 1986. Calcium-activated potassium channels and fluid secretion by exocrine glands. *Am. J. Physiol.* **251:**G1–G13

Saito, Y., Wright, E.M. 1983. Bicarbonate transport across the frog choroid plexus and its control by cyclic nucleotides. *J. Physiol. (London)* **336:**635–648

Saito, Y., Wright, E.M. 1984. Regulation of bicarbonate transport across the brush border membrane of the bull-frog choroid plexus. *J. Physiol. (London)* **350:**327–342

Sepulveda, F.V, Mason, W.T. 1985. Single channel recordings obtained from basolateral membranes of isolated rabbit enterocytes. *FEBS Lett.* **191:**87–91

Trautmann, A., Marty, A. 1984. Activation of Ca-dependent K^+ channels by carbamylcholine in rat lacrimal glands. *Proc. Natl. Acad. Sci. USA* **81:**611–615

Wright, E.M. 1977. Effect of bicarbonate and other buffers on choroid plexus Na^+/K^+ pump. *Biochim. Biophys. Acta* **468:**486–489

Zeuthen, T. 1987. The effects of chloride ions of electrodiffusion in the membrane of a leaky epithelium. *Pfluegers Arch.* **408:**267–274

Zeuthen, T., Christensen, O., Baerentsen, J.H., LaCow, M. 1987. The mechanism of electrodiffusive K^+ transport in leaky epithelia and some of its consequences for anion transport. *Pfluegers Arch.* **408:**260–266

Zeuthen, T., Wright, E.M. 1981. Epithelial potassium transport: Tracer and electrophysiological studies in choroid plexus. *J. Membrane Biol.* **60:**105–128

Received 24 November 1987; revised 13 June 1988